Slip effects on unsteady non-Newtonian blood flow through an inclined catheterized overlapping stenotic artery

Cite as: AIP Advances **6**, 015118 (2016); https://doi.org/10.1063/1.4941358
Submitted: 25 November 2015 • Accepted: 20 January 2016 • Published Online: 29 January 2016

Akbar Zaman, Nasir Ali and M. Sajid

Slip effects on unsteady non-Newtonian blood flow through an inclined catheterized overlapping stenotic artery

Akbar Zaman,[1,a] Nasir Ali,[1] and M. Sajid[2]
[1]*Department of Mathematics and Statistics, International Islamic University, Islamabad, 44000, Pakistan*
[2]*Theoretical Physics Division, PINSTECH, P. O. Nilore Islamabad 44000, Pakistan*

(Received 25 November 2015; accepted 20 January 2016; published online 29 January 2016)

Slip effects on unsteady non-Newtonian blood hydro-magnetic flow through an inclined catheterized overlapping stenotic artery are analyzed. The constitutive equation of power law model is employed to simulate the rheological characteristics of the blood. The governing equations giving the flow derived by assuming the flow to be unsteady and two-dimensional. Mild stenosis approximation is employed to obtain the reduced form of the governing equations. Finite difference method is employed to obtain the solution of the non-linear partial differential equation in the presence of slip at the surface. An extensive quantitative analysis is performed for the effects of slip parameter, Hartmann number, cathetered parameter and arterial geometrical parameters of stenosis on the quantities of interest such as axial velocity, flow rate, resistance impedance and wall shear stress. The streamlines for the blood flow through the artery are also included. [http://dx.doi.org/10.1063/1.4941358]

I. INTRODUCTION

A detail literature survey reveals that the cardiovascular disease is the most important factor in deaths. The major reason is associated with unusual hemodynamic problems within bloodstream. Theoretical knowledge of the blood circulation, hemodynamics, offers significant help in diagnosis of the coronary disease. Partial or even overall circulatory occlusion within a coronary artery lessens the bloodstream offer to the heart which in turn increase the heart attack possibilities. The accumulation of substance like cholesterol or plaque in arterial blood vessels in known as stenosis\ atherosclerosis. Catheter can be used as a tool to diagnose such type of diseases. Catheter alters the flow pattern and hemodynamics characteristics when inserted inside the artery. A glance of literature shows that several researcher have provided mathematical/theoretical studies for the blood circulation inside arteries subject to several problems. For details readers are referred to the articles by McDonald,[1] Mazumdar,[2] Fung,[3] and Zamir.[4] Kanai *et al*.[5] established that the size of catheter is directly related to the wave reflection at the catheter' tip on the basis of experimental and theoretical analysis. Back *et al*.[6] investigated the mean flow resistance of blood in arteries. They concluded that mean flow resistance of blood increases in catheterization of both normal artery and stenosed artery.

In most of the available studies blood vessels have been assumed to have zero inclination with the horizontal. This is an established fact that ducts inside the human physiological system aren't horizontal, rather have some sort of inclination. This fact encouraged researchers to investigate the blood flow in inclined arteries. Maruti Prasad and Radhakrishnachandramacharya[7] investigated the steady blood flow through inclined artery with multiple stenosis. The characteristics of the blood flow through an inclined stenotic tube have been examined by Chakraborty *et al*..[8] In other study, Sharma *et al*.[9] analyzed pulsatile MHD flow in an inclined catheterized stenosed artery with slip

[a]Corresponding author: Tel :- +92519019756 (e-mail: akbarzaman75@yahoo.com).

on the wall. They have assumed the uni-directional blood through single stenotic artery. Recently, Biswas and Paul[10] examined the suspension model for blood flow through a tapering catheterized inclined artery with asymmetric stenosis. In Refs. 7–10, the authors have assumed blood to be a Newtonian fluid. The classification of blood as a Newtonian fluid is a crude approximation because experimental results revealed that blood cannot be characterized as a Newtonian fluid.[11]

Motivated by above mentioned studies, the unsteady flow of blood flow through an inclined catheterized artery with overlapping stenosis in the presence of uniform magnetic field is considered in this paper. Furthermore the present analysis generalizes the results in Ref. 9 by taking into account non-Newtonian rheology of the streaming blood, two dimensional blood flow and the overlapping stenotic nature of the artery. The unsteady oscillatory flow considered here is a variant of flow over an oscillatory stretching sheet studied by several other authors.[12–17] The structure of the paper is as follows: Section II illustrates mathematical formulation of the problem and development of flow equations. The outline of numerical method using finite difference technique is presented in section III. Graphical results and discussions are explained in section IV. In section V, some conclusions are included.

II. MATHEMATICAL FORMULATION

Consider an incompressible fluid\blood is flowing through inclined artery of length L with overlapping stenosis subject to body force. Cylindrical coordinate system (r, θ, z) are chosen for the present analysis, where r is directed along the radial direction and z along the axial direction of an artery. The geometry for the overlapping stenosed arterial segment is defined as (see Fig. 1):

$$R(z) = \begin{cases} a\left(1 - \frac{64}{10}\eta\left(\frac{11}{32}l_0^3(z-d) - \frac{47}{48}l_0^2(z-d)^2 + l_0(z-d)^3 - \frac{1}{3}(z-d)^4\right)\right), & d \le z \le d + \frac{3}{2}l_0, \\ a, & otherwise, \end{cases} \tag{1}$$

where a is the radius of the non-tapered artery in the non-stenotic region, l_0 is the length of stenosis, d is the length of non-stenotic region and the parameter η is defined as

$$\eta = \frac{4\delta^*}{a{l_0}^4}, \tag{2}$$

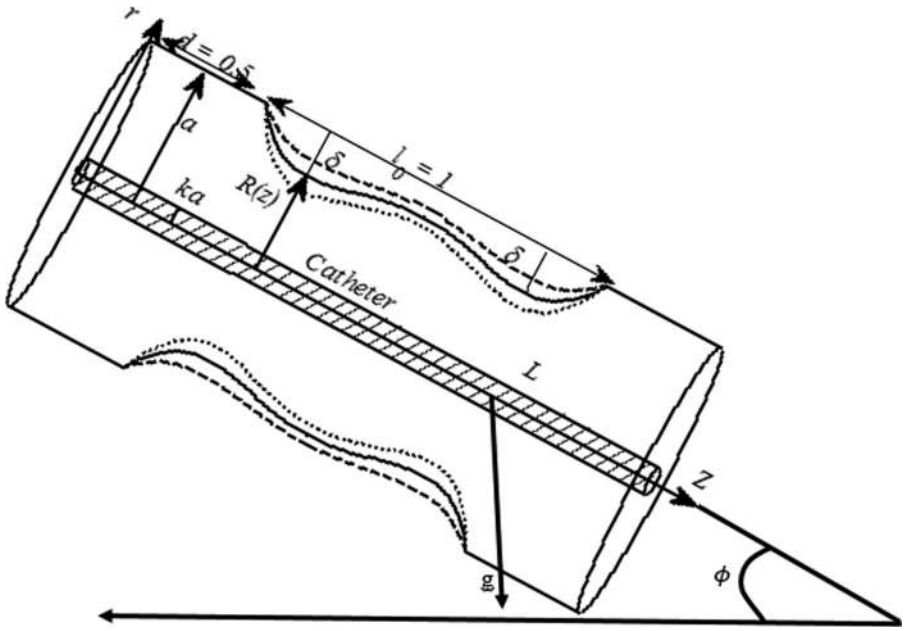

FIG. 1. Geometry of the stenosed arterial segment.

in which δ^* denotes the maximum height of the stenosis located at

$$z = d + \frac{8l_0}{25}. \tag{3}$$

The flow is governed by the following equations

$$\nabla \cdot \boldsymbol{u} = 0, \tag{4}$$

$$\rho \frac{d\boldsymbol{u}}{dt} = \nabla \cdot \boldsymbol{T} + \rho \boldsymbol{b} + \boldsymbol{J} \times \boldsymbol{B}, \tag{5}$$

where $\boldsymbol{u}$ is the blood fluid velocity, ρ is the blood density, $\boldsymbol{T}$ is the Cauchy stress tensor, $\boldsymbol{b}$ is the body force per unit volume, $\boldsymbol{J}$ is the current density, $\boldsymbol{B} = \boldsymbol{B}_0 + \boldsymbol{B}_1$ is the total magnetic field (where $\boldsymbol{B}_1$ is the induced magnetic field assumed to be negligible), $\boldsymbol{B}_0$ is the constant magnetic field applied in the radial direction[18]and d/dt is the material time derivative. By Ohm's law, we have

$$\boldsymbol{J} = \sigma \left(\boldsymbol{E} + \boldsymbol{u} \times \boldsymbol{B} \right), \tag{6}$$

where σ is the electrical conductivity of blood and $\boldsymbol{E}$ is the electric field. The imposed and induced electrical fields are assumed to be negligible and in the low magnetic Reynolds number limit we get

$$\boldsymbol{J} \times \boldsymbol{B} = -\sigma \left(\boldsymbol{u} \times \boldsymbol{B}_0 \right) \times \boldsymbol{B}_0 = -\sigma {\boldsymbol{B}_0}^2 \boldsymbol{u}. \tag{7}$$

The Cauchy stress tensor for a power law fluid is given by[19,20]

$$\boldsymbol{T} = -p\boldsymbol{I} + \boldsymbol{S}, \tag{8}$$

where

$$\boldsymbol{S} = \mu \, \Pi^{n-1} \boldsymbol{A}_1 \tag{9}$$

In which p is the pressure, $\boldsymbol{I}$ is the identity tensor, n is the power law index, μ is the dynamic viscosity of blood and $\boldsymbol{A}_1$ is the first Rivilin-Ericksen tensor, such that

$$\boldsymbol{A}_1 = \nabla \boldsymbol{u} + \nabla \boldsymbol{u}^T, \tag{10}$$

and

$$\Pi = \sqrt{\frac{1}{2} trace \left({\boldsymbol{A}_1}^2 \right)}. \tag{11}$$

It is assumed that the blood flow in the overlapping stenotic artery is unsteady, axisymmetric, laminar, two-dimensional and fully developed. Therefore the velocity field for the current analysis is given by

$$\boldsymbol{u} = \left[u(r, z, t), 0, w(r, z, t) \right]. \tag{12}$$

In view of (12), Eqs. (4) and (5) give

$$\frac{\partial u}{\partial r} + \frac{u}{r} + \frac{\partial w}{\partial z} = 0. \tag{13}$$

$$\rho \left(\frac{\partial u}{\partial t} + u \frac{\partial u}{\partial r} + w \frac{\partial w}{\partial z} \right) = -\frac{\partial p}{\partial r} + \left(\frac{1}{r} \frac{\partial}{\partial r} \left(r S_{rr} \right) + \frac{\partial}{\partial z} \left(S_{rz} \right) \right), \tag{14}$$

$$\rho \left(\frac{\partial w}{\partial t} + u \frac{\partial w}{\partial r} + w \frac{\partial w}{\partial z} \right) = -\frac{\partial p}{\partial z} + \rho g sin\left(\phi \right) + \left(\frac{1}{r} \frac{\partial}{\partial r} \left(r S_{rz} \right) + \frac{\partial}{\partial z} \left(S_{zz} \right) \right) - \sigma B_0^2 w, \tag{15}$$

$$S_{rr} = 2 \left[\mu \left\{ \left| \left[2 \left(\left(\frac{\partial u}{\partial r} \right)^2 + \left(\frac{u}{r} \right)^2 + \left(\frac{\partial w}{\partial z} \right)^2 \right) + \left(\frac{\partial u}{\partial z} + \frac{\partial w}{\partial r} \right)^2 \right] \right|^{\frac{n-1}{2}} \right\} \right] \left(\frac{\partial u}{\partial r} \right), \tag{16}$$

$$S_{zz} = 2 \left[\mu \left\{ \left| \left[2 \left(\left(\frac{\partial u}{\partial r} \right)^2 + \left(\frac{u}{r} \right)^2 + \left(\frac{\partial w}{\partial z} \right)^2 \right) + \left(\frac{\partial u}{\partial z} + \frac{\partial w}{\partial r} \right)^2 \right] \right|^{\frac{n-1}{2}} \right\} \right] \left(\frac{\partial w}{\partial z} \right), \tag{17}$$

$$S_{rz} = \left[\mu \left\{ \left| \left[2 \left(\left(\frac{\partial u}{\partial r} \right)^2 + \left(\frac{u}{r} \right)^2 + \left(\frac{\partial w}{\partial z} \right)^2 \right) + \left(\frac{\partial u}{\partial z} + \frac{\partial w}{\partial r} \right)^2 \right] \right|^{\frac{n-1}{2}} \right\} \right] \left(\frac{\partial w}{\partial r} + \frac{\partial u}{\partial z} \right). \tag{18}$$

Where angle ϕ represents the inclination angle of an artery. The boundary and initial conditions are taken as:

$$\begin{aligned} w(r,t) = V_0, u(r,t) = 0 \quad at \quad r = ka, \\ w(r,t) = \bar{U}_s, u(r,t) = 0 \quad at \quad r = R(z), \\ w(r,t) = u(r,t) = 0 \quad at \quad t = 0. \end{aligned} \tag{19}$$

Where V_0 represents the catheter velocity, k $(1 < k > 1)$ is the aspect ratio of the catheter to artery radius and $\bar{U}_s$ is the slip velocity. The above equations can be made dimensionless by defining

$$\begin{aligned} \bar{r} = \frac{r}{a}, \bar{w} = \frac{w}{V_0}, \bar{u} = \frac{l_0 u}{\delta^* V_0}, \bar{t} = \frac{\omega_p}{2\pi} t, \bar{z} = \frac{z}{l_0}, \bar{R} = \frac{R}{a}, \bar{p} = \frac{a^2 p}{V_0 l_0 \mu'}, \bar{S}_{rz} = \frac{a}{V_0 \mu'} S_{rz}, \\ \bar{S}_{rr} = \frac{l_0}{V_0 \mu'} S_{rr}, \bar{S}_{zz} = \frac{l_0}{V_0 \mu'} S_{zz}, \ \mu' = \mu \left(\frac{V_0}{a}\right)^{n-1}, e = \frac{A_1}{A_0}, \omega_r = \frac{\omega_b}{\omega_p}, U_s = \frac{\bar{U}_s}{V_0} \\ B_1 = \frac{A_0 a^2}{\mu' V_0}, B_2 = \rho A_g \frac{a^2}{\mu' V_0} = \frac{\rho A_g}{A_0} B_1, Re = \frac{\rho V_0 a}{\mu'}, \bar{g} = \frac{g}{V_0^2/a}, \end{aligned} \tag{20}$$

where ω_p is angular frequency. As an implication of these variables, Eqns. (13)-(18) after dropping bars are

$$\delta \left(\frac{\partial u}{\partial r} + \frac{u}{r}\right) + \frac{\partial w}{\partial z} = 0, \tag{21}$$

$$\alpha \delta \varepsilon^2 \left(\frac{\partial u}{\partial t} + \varepsilon Re \left(\delta u \frac{\partial u}{\partial r} + w \frac{\partial u}{\partial z}\right)\right) = -\frac{\partial p}{\partial r} + \varepsilon^2 \left(\frac{1}{r} \frac{\partial}{\partial r} (r S_{rr}) + \frac{\partial}{\partial z} (S_{rz})\right), \tag{22}$$

$$\alpha \left[\frac{\partial w}{\partial t}\right] + Re \left(\delta \varepsilon u \frac{\partial w}{\partial r} + \varepsilon^2 w \frac{\partial w}{\partial z}\right) = -\frac{\partial p}{\partial z} + \left(\frac{1}{r} \frac{\partial}{\partial r} (r S_{rz}) + \varepsilon^2 \frac{\partial}{\partial z} (S_{zz})\right) - M^2 w + Re\, g\, Sin(\phi), \tag{23}$$

$$\begin{aligned} S_{rz} = \left\{\left|\left[\left(\delta \varepsilon \left(\left(\frac{\partial u}{\partial r}\right)^2 + \left(\frac{u}{r}\right)^2\right) + \varepsilon \left(\frac{\partial w}{\partial z}\right)^2\right) + \left(\delta \frac{\partial u}{\partial z} + \frac{\partial w}{\partial r}\right)^2\right]\right|\right\}^{\frac{n-1}{2}} \left(\frac{\partial w}{\partial r} + \delta \frac{\partial u}{\partial z}\right), \\ S_{rr} = \left\{\left|\left[2\left(\delta \varepsilon \left(\left(\frac{\partial u}{\partial r}\right)^2 + \left(\frac{u}{r}\right)^2\right) + \varepsilon \left(\frac{\partial w}{\partial z}\right)^2\right) + \left(\delta \frac{\partial u}{\partial z} + \frac{\partial w}{\partial r}\right)^2\right]\right|\right\}^{\frac{n-1}{2}} \left(\varepsilon \delta \frac{\partial u}{\partial r}\right), \\ S_{zz} = \left\{\left|\left[2\left(\delta \varepsilon \left(\left(\frac{\partial u}{\partial r}\right)^2 + \left(\frac{u}{r}\right)^2\right) + \varepsilon \left(\frac{\partial w}{\partial z}\right)^2\right) + \left(\delta \frac{\partial u}{\partial z} + \frac{\partial w}{\partial r}\right)^2\right]\right|\right\}^{\frac{n-1}{2}} \left(\varepsilon \frac{\partial w}{\partial z}\right). \end{aligned} \tag{24}$$

We have assumed the stenosis to be mild ($\delta = \delta^*/a << 1$), and the ratio$\varepsilon = a/l_0 \approx O(1)$. In view of the above assumptions, Eqns. (22) - (23) reduce to

$$\frac{\partial p}{\partial r} = 0, \tag{25}$$

$$\alpha \left[\frac{\partial w}{\partial t}\right] = -\frac{\partial p}{\partial z} + \frac{1}{r} \frac{\partial}{\partial r} \left[r \left|\frac{\partial w}{\partial r}\right|^{n-1} \frac{\partial w}{\partial r}\right] - M^2 w + Re\, g \sin(\phi), \tag{26}$$

to gather with the pressure gradient[21] in dimensionless form

$$-\frac{\partial p}{\partial z} = B_1 (1 + e cos(2\pi t)), \tag{27}$$

where $\alpha = \rho \omega a^2 / 2\pi \mu'$ is the *Wormsley number*, B_1 is the amplitude of the pulsatile parameter and $M = B_0 a (\sigma/\mu')^{1/2}$ is the Hartmann number.

Using value of $-\partial p/\partial z$ in axial momentum equation (26), we get

$$\alpha \left[\frac{\partial w}{\partial t}\right] = B_1 (1 + e cos(2\pi t)) + \frac{1}{r} \frac{\partial}{\partial r} \left[r \left|\frac{\partial w}{\partial r}\right|^{n-1} \frac{\partial w}{\partial r}\right] - M^2 w + Re\, g \sin(\phi), \tag{28}$$

$$w(r,t) = 1, \quad at \quad r = k,$$
$$w(r,t) = U_s, \quad at \quad r = R(z), \tag{29}$$

Volumetric flow rate, the shear stress at the wall and resistance to flow or impendence in terms of this new variables are

$$Q = \int_0^1 ur\,dr, \tag{30}$$

$$\tau_s = \left(\left| \frac{\partial u}{\partial r} \right|^{n-1} \frac{\partial u}{\partial r} \right)_{r=1}, \tag{31}$$

$$\lambda = \frac{L\left(\frac{\partial p}{\partial z}\right)}{Q}. \tag{32}$$

The dimensionless form of geometry equation is given by:

$$R(z) = (1+\xi z)\left[1 - \frac{64}{10}\eta_1\left(\frac{11}{32}(z-\sigma) - \frac{47}{48}(z-\sigma)^2 + (z-\sigma)^3 - \frac{1}{3}(z-\sigma)^4\right)\right], \quad \sigma \le z \le \sigma + 1.5,$$
$$\text{where} \quad \eta_1 = 4\delta,\ \delta = \frac{\delta^*}{a}, \sigma = \frac{d}{l_0},\ \xi = \frac{\xi' l_0}{a}. \tag{33}$$

The radial coordinate transformation[22] is used in momentum to incorporate the geometry effects,

$$x = \frac{r}{R(z)}, \tag{34}$$

using Eq. (34) in Eq. (28) and (29), we get

$$\alpha\left[\frac{\partial w}{\partial t}\right] = B_1(1 + ecos(2\pi t)) + \frac{1}{xR^{n+1}}\frac{\partial}{\partial x}\left[x\left|\frac{\partial w}{\partial x}\right|^{n-1}\frac{\partial w}{\partial x}\right] - M^2 w + g\sin(\phi), \tag{35}$$

$$w(x,t)|_{x=k} = 1,\ w(x,t)|_{x=1} = U_s. \tag{36}$$

Similarly the volumetric flow rate, the shear stress at the wall and resistance impendence respectively takes the form:

$$Q = R^2\left(\int_0^1 w\,x dx\right), \tag{37}$$

$$\tau_w = \frac{1}{R^n}\left(\left|\frac{\partial w}{\partial x}\right|^{n-1}\frac{\partial w}{\partial x}\right)_{x=1}, \tag{38}$$

$$\lambda = \frac{\frac{L}{l_0}\left(\frac{\partial p}{\partial z}\right)}{Q}, \tag{39}$$

Substituting the value dimensionless form of pressure gradient in Eq. (40), we can write,

$$\lambda = \frac{L}{l_0}\frac{B_1(1 + ecos(2\pi t))}{\left(\int_0^1 w\,x dx\right)R(z)}. \tag{40}$$

III. NUMERICAL SOLUTION USING FINITE DIFFERENCE METHOD

Finite difference scheme has been incorporated[23–25] to obtain the numerical solution of Eq. (35) subject to boundary and initial conditions (36). In this scheme, radial derivative is approximated by *central* difference formulae while *time* derivative is approximated by a *forward* difference formula.

The notation w_i^j is used to represent the value of w at node x_i and at time instant t_j. Thus, we write

$$\frac{\partial w}{\partial x} \cong \frac{w_{i+1}^j - w_{i-1}^j}{2\Delta x} = w_x, \tag{41}$$

$$\frac{\partial^2 w}{\partial x^2} \cong \frac{w_{i+1}^j - 2w_i^j + w_{i-1}^j}{(\Delta x)^2} = w_{xx}, \tag{42}$$

and

$$\frac{\partial w}{\partial t} \cong \frac{w_i^{j+1} - w_i^j}{\Delta t}. \tag{43}$$

Using the above approximation for spatial and time derivatives in (35), we get the following difference equation:

$$w_i^{j+1} = w_i^j + \frac{dt}{\alpha}\left[B_1\left(1 + ecos(2\pi t^j)\right) + \frac{1}{xR^{n+1}}|w_x|^{n-1}w_x + \frac{w_x}{R^{n+1}}\frac{\partial}{\partial x}\left(|w_x|^{n-1}\right) + \frac{1}{R^{n+1}}|w_x|^{n-1}w_{xx} - M^2 w_i^j + Re\, g \sin(\phi)\right] \tag{44}$$

The finite difference representation of the prescribed conditions is given by

$$\begin{aligned} w_i^1 &= 0, && at\ t = 0, \\ w_{N+1}^j &= U_s, && at\ x = 1, \\ w_i^j &= 1 && at\ x = k. \end{aligned} \tag{45}$$

The numerical solution is sought for $N + 1$ uniformly discrete points $x_i, (i = 1, 2, \ldots . N + 1)$ with a grid size $\Delta x = {}^1/_{N+1}$ at the time levels $t_j = (j - 1)\Delta t$, where Δt is the small increment in time. To obtain the accuracy of the order $\sim 10^{-7}$, we have taken the following step sizes: $\Delta x = 0.025$ and $\Delta t = 0.00001$.

IV. RESULTS AND DISCUSSION

In this section graphical results are displayed for the following set of parameters: $d = 0.5$, $l_0 = 1.0$, $\omega_p = 2\pi f_p$, $f_p = 1.2$, $\omega_b = 2\pi f_b$, $Re = 1$.

Fig. 2 illustrate dimensionless velocity profiles for different values of slip velocity (U_s) panel (a) and inclination parameter ϕ panel (b), where τ_s is the dimensionless steady state time at which the maximum velocity is obtained. This figure indicates that magnitude of axial velocity increases by increasing both of slip velocity or inclination angle. It is therefore concluded that increasing either of slip velocity or inclination angle accelerate the flow ad results in larger momentum flux through the whole arterial segment.

The dimensionless velocity profiles for different values of Hartmann number (M) and dimensionless catheter radius (k) are shown in Fig. 3(a) and 3(b) respectively. It is found that in the

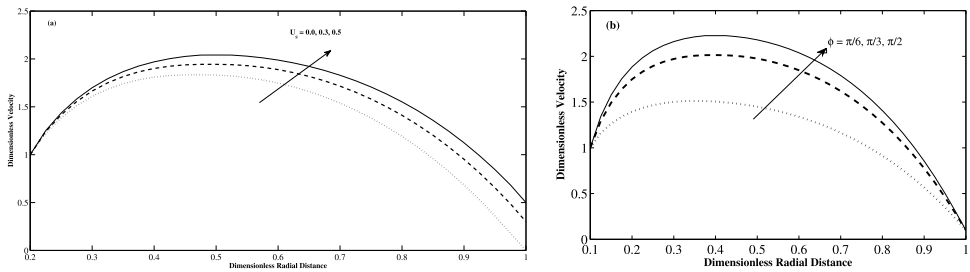

FIG. 2. (a) Velocity profile for different values of slip parameter U_s and Fig. 2. (b) angle of inclination ϕ with the following data: $t = \tau_s$, $z = 0.77$, $\alpha = 2, e = 0.2$, $\delta = 0.1$, $n = 0.8, k = 0.1, M = 0.5$.

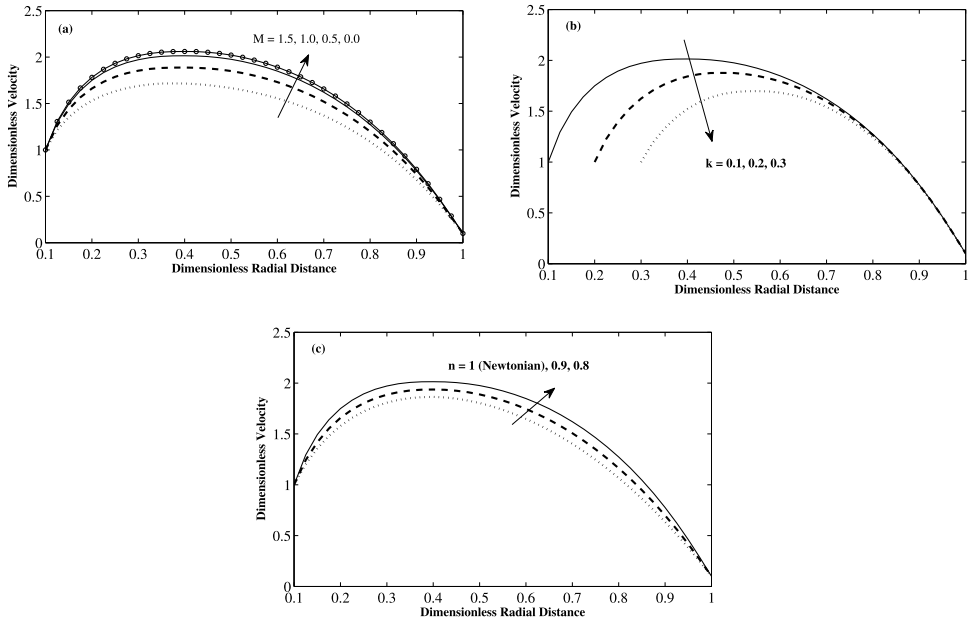

FIG. 3. (a) Velocity profile for different values of Hartmann number, Fig. 3. (b) size of catheter radius and Fig. 3. (c) power law parameter n with the following data: $t = \tau_s$, $z = 0.77$, $\delta = 0.1$, $\alpha = 2, e = 0.2, k = 0.1$, $n = 0.8$, $\phi = \pi/3, U_s = 0.1$.

present scenario the axial velocity of the blood decreases with increasing the strength of the applied magnetic field or the catheter radius. In fact, under the considered conditions the magnetic force is a resistance to flow, and its magnitude is proportional to the axial velocity of blood, hence a flow declaration is observed with the increase of M. In the same way, the drag force experienced by the streaming blood increases with the increase of catheter radius and hence the amplitude of flow near the catheter radius substantially. The variation in axial velocity for various values of power law parameter n is shown in Fig. 3(c). As expected the magnitude of flow velocity increases with a change in the behavior of the blood from Newtonian to shear thinning. This trend is physically realizable because of decrease in the effective viscosity of the blood for $n < 1$.

The plots of dimensionless flow rate at the stenotic throat ($z = 0.77$) for different values of M *and* k in the stenotic region are shown in Figs. 4(a) and 4(b). These figure reveals that flow rate decreases with increasing the strength of the magnetic field or the radius size of catheter, which shows that the effect of these parameters is to diminish the magnitude of flow rate.

The influence of slip parameter U_s and inclination parameter ϕ on dimensionless flow rate in the stenotic region is illustrated through Figs. 5(a) and 5(b). It is evident that flow rate increases with an increase in the magnitude of slip parameter or inclination angle. The behavior of the flow rate is directly linked with the behavior of the velocity. If velocity is an increasing (or decreasing) function

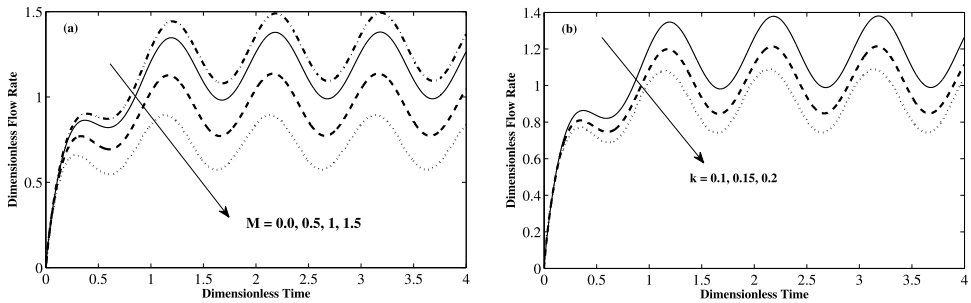

FIG. 4. (a) Flow rate for different values of Hartmann number,M and Fig. 4. (b)k with the following data: $z = 0.77, \mathrm{U}_s = 0.1, \phi = \pi/3$, $\alpha = 1, e = 1$, $\delta = 0.1$.

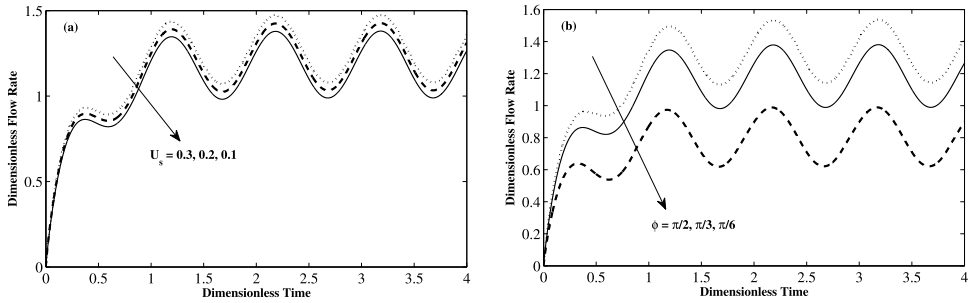

FIG. 5. (a) Flow rate for different values of ϕ and Fig. 5. (b) U_S with the following data: $z = 0.77, n = 0.8$, $k = 0.1$, $\alpha = 1, e = 1, M = 0.5, U_s = 0.1$.

of a certain parameter than so is the case with flow rate. Therefore, increasing (decrease) in flow rate with increasing slip velocity and inclination angle (Hartmann number and catheter radius) is a direct consequence of increase (decrease) in velocity with increasing these parameters.

The profiles of wall shear stress at the stenotic throat ($z = 0.77$) for different values of Hartmann number, and catheter radius are shown in Figs. 6(a) and 6(b), respectively. Fig. 6(a) indicates that wall shear stress decreases from the purely hydrodynamic (non-magnetic) to the magneto-hydrodynamic case, since the presence of magnetic field decelerates the flow and reduces wall stress. Fig. 6(b) depicts a similar behavior of wall shear stress with increasing the catheter radius as observed through Fig. 6(a).

The time-series of dimensionless wall shear stress at the stenotic throat ($z = 0.77$) for different values of slip parameter U_s is shown in Fig. 7(a). It is evident from inspection of Fig. 7(a) that an increase in the slip parameter U_s decreases the magnitude of the wall shear stress. Similarly wall shear stress at the stenotic throat follows an increasing trend with increasing the angle of inclination. It is therefore concluded through Fig. 7 that flow acceleration caused by increasing the angle of inclination at the stenotic throat increases the wall shear stress there. In contrast, the flow acceleration caused by slippage at the stenotic throat reduces the wall shears stress there.

The time-series of dimensionless resistance to flow of various values of inclination angle and slip parameter is plotted in Fig. 8(a) and 8(b). It is noted that resistance to flow decreases with increase in the magnitude of angle of inclination or slip parameter.

The blood flow patterns over for the whole arterial segment at time instant $t = 0.45$ (which belongs to diastolic phase) are shown in Fig. 9 (Panels (a)-(d)). Panel (a) is considered as standard and rest of the panels are compared with it in order to illustrate the effects of various parameters on bolus pattern. Panels (a) and (b) illustrate streamlines for $\phi = \pi/3$ and $\phi = \pi/2$, respectively. Both panels indicate a circulating bolus of fluid in the overlapping stenosed region of the artery and their comparison reveals a decrease in the size of bolus by increasing the angle of inclination. The effect of slip parameter on streamlines pattern can be observed through the comparison of panels (a) and (c). It is observed that an increase in the strength of slip parameter decreases the size of

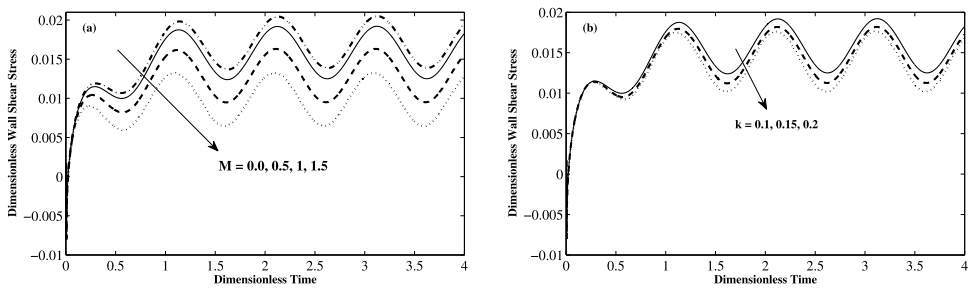

FIG. 6. (a) Dimensionless wall shear stress for different values of Hartmann number, M and Fig. 6. (b) k with the following data: $z = 0.77$, $U_S = 0.1$, $\phi = \pi/3$, $\delta = 0.1$.

the circulating bolus. This is perhaps due to the accelerating effect of slip on the flow velocity. Finally, a comparison of panels (a) and (d) illustrates the effects of catheter radius on streamlines pattern. It clear that size and circulation of trapped bolus decreases when the radius of the catheter is increased.

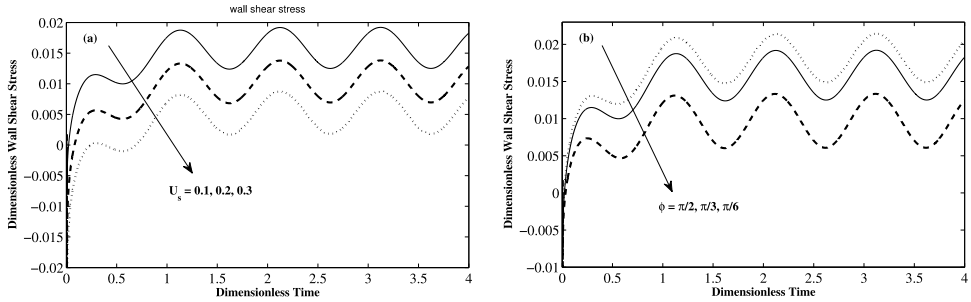

FIG. 7. (a) Wall shear stress for different values of U_s and Fig. 7. (b) ϕ with the following data: $z = 0.77, n = 0.8$, $k = 0.1$, $M = 0.5, U_s = 0.1$.

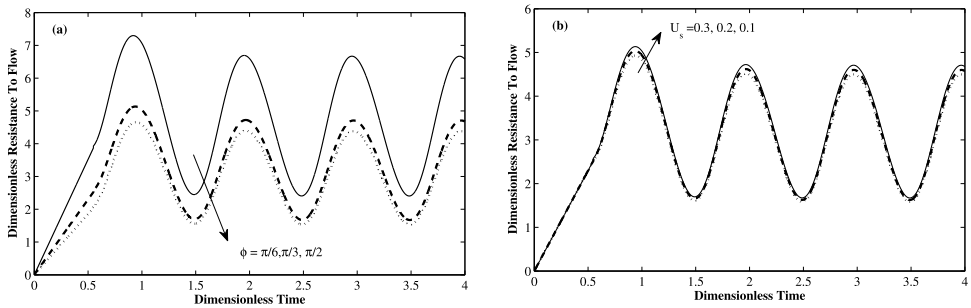

FIG. 8. (a) Resistance to flow for different values of permeability parameter ϕ and Fig. 8. (b)U_s with the following data: $z = 0.77, n = 0.8$, $k = 0.1$, $M = 0.5, U_s = 0.1$.

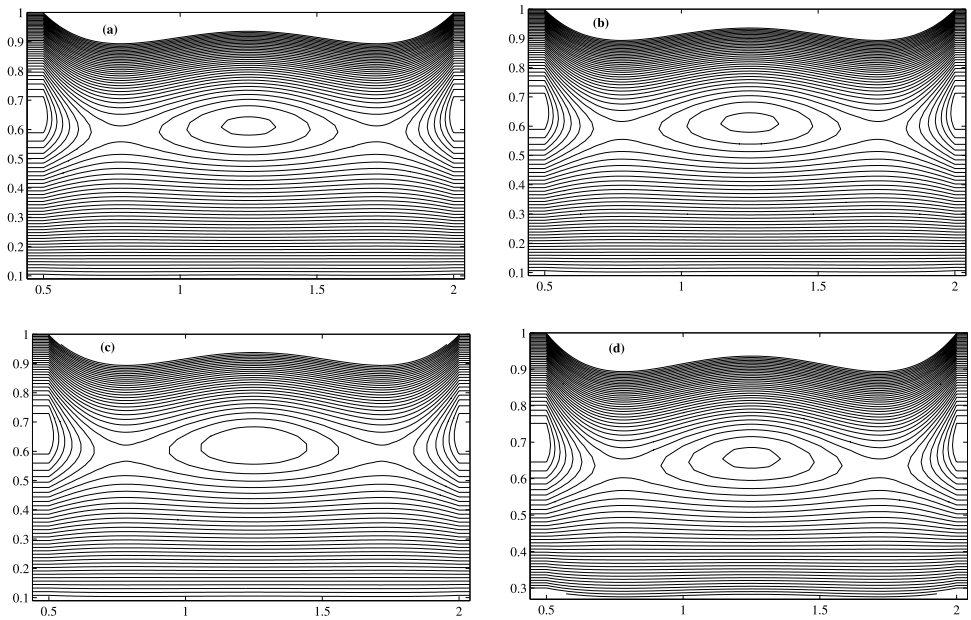

FIG. 9. (a)-(d) Blood flow patterns for: $\delta = 0.1$, $B_1 = 4$, $t = 0.45$.

V. CONCLUSIONS

A mathematical model for magneto-hydrodynamic pulsatile flow of blood through overlapping stenotic artery incorporating the effects of inclination angle and slip is presented. The Constitutive model equation of non-Newtonian power-law model is used to characterize the blood rheology. The nonlinear partial differential equation for the model under consideration is derived employing the laws of mass and momentum conservation. The solution is obtained using an explicit finite difference scheme. The numerical results show that the wall slip and inclination angle of the artery have significant effects on the hemodynamical variables like axial velocity, flow rate, wall shear stress and resistance impedance. In fact these variables, except wall shear stress, follow a similar trend by increasing slip parameter or inclination angle. However, the behavior of wall shear stress with increasing the slip parameter is quite opposite to the behavior of the wall shear stress with increasing the inclination angle. Moreover, the streamlines of the flow also follow a similar trend with increasing slip at the wall or inclination angle of the arterial segment.

[1] D.A. McDonald, *Blood flow in arteries* (Arnold, London, 1960).
[2] J. N. Mazumdar, *bio-fluid mechanics* (Word Scientific Press, 1992).
[3] Y.C. Fung, *Biodynamics Circulation* (Springer-Verlag, New York, 1984).
[4] M. Zamir, *The physics of coronary blood flow* (Springer, New York, 2005).
[5] H. Kanai, M. Lizuka, and K. Sakamotos, "One of the problem in the measurement of blood pressure by catheterization: Wave reflection at the tip of catheter," Medical & Biological Engineering **28**, 483-496 (1996).
[6] L. H. Back, E.Y. Kwack, and M. R. Back, "Flow rate-pressure drop relation in coronary angioplasty: catheter obstruction effect," Journal of Biomechanical Engineering **118**, 83-89 (1996).
[7] K. M. Prasad and G. Radhakrishnamcharya, "Flow of herschel-bulkley fluid through an inclined tube of non-uniform cross-section with multiple stenoses," Arch. Mech. **60**, 161-172 (2008).
[8] U. S. Chakraborty, D. Biswas, and M. Paul, "Suspension model blood flow through an inclined tube with an axially non-symmetrical stenosis," Korea-Australia Rheol. J. **23**, 25-32 (2011).
[9] M. K. Sharma, K. Singh, and S. Bansal, "Pulsatile MHD flow in an inclined catheterized stenosed artery with slip on the wall," J. Biomed. Sci. and Engg **7**, 194-207 (2014).
[10] D. Biswas and M. Paul, "Suspension model for blood flow through a tapering catheterized inclined artery with asymmetric stenosis," Applic. Appl. Math. I. J. **10**, 474–495 (2015).
[11] H. A. Branes, J. F. Hutton, and K. Walter, *An introduction to rheology* (Elsevier, Amsterdam, 1989).
[12] "Unsteady MHD free convection flow of Casson fluids past over an oscillating vertical plate embedded in a porous medium," A. Khalid, I. Khan, A. Khan, and S. Shafie, Engineering Science and Technology: An International Journal **18**, 309-317 (2015).
[13] Nasir Ali, Sami Ullah Khan, and Zaheer Abbas, "Hydromagnetic Flow and Heat Transfer of a Jeffrey Fluid over an Oscillatory Stretching Surface," Zeits. Naturfor. A. **70**, 2014-0273 (2015).
[14] "Exact Solutions for unsteady free convection flow of Casson fluid over an oscillating vertical plate with constant wall temperature," A. Khalid, I. Khan, and S. Shafie, J. Abstract Appl. Analys. ID 946350 (2015).
[15] Sami Ullah Khan, Nasir Ali, and Zaheer Abbas, "Hydromagnetic Flow and Heat Transfer over a Porous Oscillating Stretching Surface in a Viscoelastic Fluid with Porous Medium," PLoS ONE 12/2015 **10**(12).
[16] "Conjugate transfer of heat and mass in unsteady flow of a micropolar fluid with wall couple stress," A. Khalid, I. Khan, A. Khan, and S. Shafie, AIP Advances. **5**, 127125 (2015).
[17] Z. abbas, Y. Wang, T. Hayat, and M. Oberlack, "Hydromagnetic flow in a viscoelastic fluid due to the oscillatory stretching surface," Int. J. Non Linear Mech. **43**, 783-793 (2008).
[18] M. A. Ikbal, S. Chakravarty, K. K. L. Wong, J. Mazumdar, and P. K. Mandal, "Unsteady response of non-Newtonian blood flow through a stenosed artery in magnetic field," J. Comput. Appl. Math. **230**, 243-259 (2009).
[19] F. Yilmaz and M. Y. Gundogdu, "A critical review on blood flow in large arteries; relevance to blood rheology, viscosity models, and physiologic conditions, Korea-Australia," Rheol. J. **20**, 197-211 (2008).
[20] A. Zaman, N. Ali, and O. A. Bég, "Unsteady magnetohydrodynamic blood flow In a porous-saturated overlapping stenotic artery: numerical modeling," J. Mech. Med. Bio. **16**, 16 (2015).
[21] A. Zaman, N. Ali, M. Sajid, and T. Hayat, "Effects of unsteadiness and non-Newtonian rheology on blood flow through a tapered time-variant stenotic artery," AIP Advances **5**, 037129 (2015).
[22] SC Ling and HB Atabek, "A nonlinear analysis of pulsatile flow in arteries," J Fluid Mech **55**, 493–511 (1972).
[23] N. Ali, A. Zaman, M. Sajid, J. J. Nietoc, and A. Torres, "Unsteady non-Newtonian blood flow through a tapered overlapping stenosed catheterized vessel," Math. Bio-sci. **269**, 94–103 (2015).
[24] K. A. Hoffmann and S. T. Chiang, *Computational Fluid Dynamics* (Engineering Edition System, Wichita, Kansas USA, 2000), Vol. 1, pp. 67208-1078.
[25] P. K. Mandal, "An unsteady analysis of non-Newtonian blood through tapered arteries with a stenosis," Int. J. Nonlinear. Mech. **40**, 151–164 (2005).